ROYAL SOCIETY
OF CHEMISTRY

PAPER
Jaewook Lee, Sungwhan An *et al.*
Formulation of lipid nanoparticles containing
ginsenoside Rg2 and protopanaxadiol for highly
efficient delivery of mRNA

European
Society for
Biomaterials

Biomaterials Science

PAPER

Check for updates

Formulation of lipid nanoparticles containing ginsenoside Rg2 and protopanaxadiol for highly efficient delivery of mRNA†

Sin A Park,‡[a] Dajeong Hwang, [iD] ‡[a] Jae Hoon Kim,[a] Seung-Yeul Lee,[a] Jaebeom Lee, [iD] [b,c] Han Sang Kim,[d,e] Kyung-A Kim, [iD] [e] Bumhee Lim,[f] Jae-Eon Lee,[g] Yong Hyun Jeon,[g] Tae Jeong Oh, [iD] [a] Jaewook Lee [iD] *[a] and Sungwhan An [iD] *[a]

Lipid nanoparticles (LNPs) are widely recognized as crucial carriers of mRNA in therapeutic and vaccine development. The typical lipid composition of mRNA-LNP systems includes an ionizable lipid, a helper lipid, a polyethylene glycol (PEG)-lipid, and cholesterol. Concerns arise regarding cholesterol's susceptibility to oxidation, potentially leading to undesired immunological responses and toxicity. In this study, we formulated novel LNPs by replacing cholesterol with phytochemical-derived compounds, specifically ginsenoside Rg2 and its derivative phytosterol protopanaxadiol (PPD), and validated their efficacy as mRNA delivery systems. The mRNA–LNP complexes were manually prepared through a simple mixing process. The biocompatibility of these Rg2-based LNPs (Rg2-LNP) and PPD-based LNPs (PPD-LNP) was assessed through cell viability assays, while the protective function of LNPs for mRNA was demonstrated by RNase treatment. Enhanced green fluorescent protein (EGFP) mRNA delivery and expression in A549 and HeLa cells were analyzed using optical microscopy and flow cytometry. The expression efficiency of Rg2-LNP and PPD-LNP was compared with that of commercially available LNPs, with both novel formulations demonstrating superior transfection and EGFP expression. Furthermore, *in vivo* tests following intramuscular (I.M.) injection in hairless mice demonstrated efficient *luciferase* (*Luc*) mRNA delivery and effective Luc expression using Rg2-LNP and PPD-LNP compared to commercial LNPs. Results indicated that the efficiency of EGFP and Luc expression in Rg2-LNP and PPD-LNP surpassed that of the cholesterol-based LNP formulation. These findings suggest that Rg2-LNP and PPD-LNP are promising candidates for future drug and gene delivery systems.

[a]*Genomictree Inc., Yuseong-gu, Daejeon, 34027, Republic of Korea.
E-mail: jwlee@genomictree.com, sungwhan@genomictree.com*
[b]*Department of Chemistry, Chungnam National University, Yuseong-gu, Daejeon, 34134, Republic of Korea*
[c]*Department of Chemical Engineering and Applied Chemistry, Chungnam National University, Yuseong-gu, Daejeon, 34134, Republic of Korea*
[d]*Yonsei Cancer Center, Division of Medical Oncology, Department of Internal Medicine, Yonsei University College of Medicine, Seoul, Republic of Korea*
[e]*Department of Internal Medicine, Graduate School of Medical Science, Brain Korea 21 Project, Yonsei University College of Medicine, Seoul, Republic of Korea*
[f]*New Drug Development Center, Daegu-Gyeongbuk Medical Innovation Foundation (K-MEDIhub), Dong-gu, Daegu, 41061, Republic of Korea*
[g]*Preclinical Research Center, Daegu-Gyeongbuk Medical Innovation Foundation (K-MEDIhub), Dong-gu, Daegu, 41061, Republic of Korea*
†Electronic supplementary information (ESI) available. See DOI: https://doi.org/10.1039/d4bm01070a
‡Both contributed equally.

Introduction

Recently, mRNA-based gene therapeutics and vaccines have garnered significant attention due to their numerous advantages, including the facile development of medicines for diseases induced by specific genes and the ability to tune target protein production in the body for therapeutic purposes.[1–5] This has led to a rapid expansion of approved mRNA-based drugs.[6] However, for therapeutic efficacy, mRNA must penetrate target cells and accurately translate proteins. Thus, the development of effective delivery systems is crucial.[7–9]

Lipid nanoparticles (LNPs) stand out as notable vehicles that have significantly advanced mRNA applications in humans, with several mRNA-based therapies either approved or in clinical trials.[10] Various mRNA delivery systems have been developed, including viral vectors like adeno-associated virus (AAV), lentivirus (LV) and non-viral carriers such as lipid nanoparticles (LNPs), liposomes, exosomes, polyol-based NPs, and inorganic NPs like gold or magnetic NPs.[11–16] In most

cases, LNP-based mRNA delivery systems have been widely used, and the FDA has approved those complex structure-based COVID-19 vaccines from Moderna and Pfizer/BioNTech.[17–20] Typically, LNPs are composed of four essential components: an ionic lipid, helper lipid, PEG lipid, and sterol, and they have a specific role in structural formation. Among these, sterol is important in maintaining the lipid bilayer structure, enhancing the nanostructure stability and mRNA protection.[21–24] Although cholesterol is commonly used as the sterol component, its application poses certain risks.[25–28] Because cholesterol is easily oxidized and converted to oxidative derivatives, including oxysterols like 25-hydroxycholesterol and 7β-hydroxycholesterol, it exhibits potential toxicity.[29–31] Moreover, it is possible that there is a risk of unexpected virus contamination because of animal-derived cholesterol.[32]

In this study, we have developed an alternative LNP formulation that replaces cholesterol with ginsenoside, Rg2, or its derivative phytosterol, protopanaxadiol (PPD), to address such issues. These new formulations, abundant in ginseng, mitigate the risks associated with cholesterol and leverage the significant bioactivity and biocompatibility of these phytochemicals, including anti-cancer and antioxidant effects.[33–36] These beneficial properties make them suitable components for LNP formulation, with potentially synergistic effects alongside mRNA therapeutics.[37–39] For therapeutic efficacy, mRNA needs to penetrate target cells and translate proteins adequately. In the present study, we have evaluated new LNPs that were Rg2-based LNPs (Rg2-LNP) and PPD-based LNPs (PPD-LNP) regarding their low toxicity, high biocompatibility, and mRNA protection ability against RNase. Also, we have demonstrated their effectiveness as a carrier for mRNA delivery and expression *in vitro* using enhanced green fluorescent protein (EGFP) mRNA as well as *in vivo* using *luciferase* (*Luc*) mRNA. Overall, the results described here show that ginsenoside and phytosterol-based LNPs could be alternatives to cholesterol-based LNPs, and consequently, Rg2-LNP and PPD-LNP exhibited considerable potential as delivery systems for mRNA therapeutics and vaccines.

Materials and methods

Materials and instruments

Ginsenoside Rg2, phytosterol protopanaxadiol (PPD), heptadecan-9-yl 8-[2-hydroxyethyl-(6-oxo-6-(undecyloxy)hexyl)amino]octanoate (ionizable lipid), 1,2-dioleoyl-*sn*-glycero-3-phosphoethanolamine (DOPE, phospholipid), and 1,2-dimyristoyl-*rac*-glycero-3-methoxypolyethylene glycol-2000 (PEG lipid) were purchased from Cayman Chemical (Ann Arbor, MI, USA). Also, as the positive control of LNPs, commercially available LNP preparation kits (the SM-102-LNP kit and ALC-0315-LNP kit) were purchased from Cayman Chemical. The SM-102 LNP kit contains SM-102 (ionizable lipid), distearoylphosphatidylcholine (DSPC, helper lipid), PEG lipid and cholesterol. SM-102-LNP was used for COVID-19 mRNA vaccine formulation in

Moderna. We also used the ALC-0315 LNP kit to produce the other positive control LNP and it is composed of ALC-0315 (ionizable lipid), DSPC, PEG lipid and cholesterol. This LNP was also formulated for COVID-19 mRNA vaccine in Pfizer/BioNTech. RPMI, DMEM, FBS, and penicillin–streptomycin were purchased from Well Gene (Gyeongsan, Gyeongsangbuk-do, South Korea) and plates were bought from Thermo Fisher Scientific (Waltham, Massachusetts, USA) for cell culture. A549 and HeLa cells were purchased from the Korean Cell Line Bank (Seoul, South Korea). A Quant-iT Ribogreen RNA assay kit was bought from Invitrogen/Thermo Fisher Scientific (Seoul, South Korea). The *in vitro* luciferase assay kit was purchased from Promega (Madison, WI, USA).

The size and morphology of Rg2-LNP and PPD-LNP were characterized using a nanoparticle tracking analyzer (NTA, NanoSight NS300, Malvern Panalytical, Malvern, UK), a zetasizer (Nano ZS, Malvern Panalytical, Malvern, UK) for measurement of dynamic light scattering (DLS) and a transmission electron microscope (TEM, H-7600, Hitachi, Tokyo, Japan). The cell morphology and expression of EGFP after EGFP mRNA delivery into the cell were monitored using a fluorescence optical microscope (Olympus, CKX553, Tokyo, Japan). The cell viability was measured using cell counting kit-8 (CCK-8) from Dojindo (Kumamoto, Kyushu, Japan), and the absorbance was measured using a microplate spectrophotometer (Mobi, MicroDigital, Seongnam, South Korea). The fluorescence (FL) intensity was monitored using a microplate multi-mode reader (Bio Tek Synergy HTX, Agilent, Santa Clara, CA, USA). The EGFP positive cells and the mean of FL intensities were characterized by flow cytometry (BD FACSLyric™, BD Biosciences, Franklin Lakes, NJ, USA). Male Balb/c nude mice were purchased (Orient Bio Inc, Seongnam, South Korea), and live animal imaging was performed using an IVIS Lumina III imaging system (PerkinElmer, Waltham, MA, USA).

Methods

mRNA design encoding EGFP and *luciferase*. Sequences of 5′ and 3′-un-translational region (UTR) of mRNAs encoding EGFP and *Luc* were derived from UTR sequences of sub-genomic RNA encoding nucleocapsid of SARS-Cov2.[40] The detailed procedure of production of mRNA encoding EGFP and *Luc* is described in the supplementary methods. In addition, a schematic illustration of the production and the result of gel electrophoresis of EGFP mRNA and *Luc* mRNA is depicted in Fig S1.†

Preparation of Rg2-LNP and PPD-LNP. Rg2-LNP and PPD-LNP were synthesized in absolute ethanol through a manual mixing method. Firstly, to produce the Rg2-LNP, heptadecanoic-9-yl 8-[2-hydroxyethyl-(6-oxo-6-(undecyloxy)hexyl)amino]octanoate (ionizable lipid, SM-102), 1,2-dioleoyl-*sn*-glycero-3-phosphoethanolamine (phospholipid, DOPE), 1,2-dimyristoyl-*rac*-glycero-3-methoxypolyethylene glycol-2000 (PEG lipid) and Rg2 were gently mixed in 500 μL of ethanol with several molar ratios, 50 : 10 : 1.5 : 78 or 50 : 10 : 1.5 : 39 (molar ratio = ionizable lipid : phospholipid : PEG lipid : Rg2). Subsequently, Rg2-LNP was softly mixed with mRNA to con-

struct the mRNA-Rg2-LNP complex for the delivery and expression test under various weight ratios (wmRNA : wLNP), 1 : 5, 1 : 10 and 1 : 20, and that the mixture was incubated for 15 min at room temperature (R.T.). In this case, the solvent volume ratio (VmRNA : VLNP) between aqueous solution (mRNA) and ethanol (LNP) was 3 : 1. After incubation, the mRNA-Rg2-LNP was sonicated for 1 min and then treated with the cell to evaluate the delivery and expression efficiency.

To synthesize the PPD-LNP, components for the LNP formulation were mixed under varying concentrations: 50 : 10 : 1.5 : 45.8 and 50 : 10 : 1.5 : 22.9 (molar ratio = ionizable lipid : phospholipid : PEG lipid : PPD). The mRNA : PPD-LNP mixing ratio for further study was the same as for Rg2-LNP.

To evaluate the encapsulation efficiency of Rg2-LNP and PPD-LNP using the Ribogreen RNA assay kit, the FL intensity was measured with a microplate multi-mode reader at an excitation wavelength of 480 nm and an emission wavelength of 530 nm.

Cell culture. Lung cancer cell lines (A549) and cervical carcinoma cell lines (HeLa) were grown in cell culture plates for the cytotoxicity test. Each cell line was cultured in RPMI medium and DMEM mixed with 10% FBS and penicillin–streptomycin in a 37 °C incubator under 5% CO_2 conditions.

Cytotoxicity test. Initially, A549 or HeLa cells were seeded around 7×10^3 cells per well in 96 well plates. Next, to confirm the biocompatibility of the carrier, each cell line was treated with 0.05 μg of Rg2-LNP or PPD-LNP under several concentration conditions. Then, cells were cultured in an incubator at 37 °C under 5% CO_2 for 24 h. Afterward, the cell viability was determined by the CCK assay, according to the manufacturer's instructions. After treatment with the assay reagent and further incubation for 1 h, the absorbance was measured at 450 nm using a microplate reader to confirm the relative cell viability. Additionally, dose-dependent cell viability for A549 and HeLa cells was analyzed with concentrations ranging from 0.025 μg to 0.1 μg under the same conditions.

LNP-mRNA protection test against RNase. To assess the stability of mRNA encapsulated in the LNP against RNase, 1 μg of naked EGFP mRNA and 1 μg of EGFP mRNA-encapsulated Rg2-LNP or PPD-LNP were mixed with 0.01 μg, 0.005 μg, and 0.0025 μg of RNase to conduct a test on the stability of mRNA encapsulated in the LNP. After treatment with RNase, the sample was incubated at 37 °C for 1 h, and then Proteinase K was added to the mixture and incubated continuously for 10 min to inactivate the RNase. After that, the naked mRNA and mRNA encapsulated in LNPs were analyzed by agarose gel electrophoresis (1.5%, 0.5 × TBE buffer).

In vitro test for EGFP mRNA delivery and expression. To analyze the efficiency of delivery and expression of the EGFP mRNA-contained Rg2-LNP and PPD-LNP, 250 ng of EGFP mRNA encapsulated into each LNP under the above formulation conditions were treated with A549 or HeLa cells seeded around 0.05×10^6 cells per well in a 24-well plate. To compare the EGFP expression between Rg2-LNP or PPD-LNP and commercially available LNPs (SM-102-LNP and ALC-0315-LNP) containing cholesterol, the same amount of *EGPF* mRNA was

encapsulated into SM-102-LNP or ALC-0315-LNP or modified SM-102-LNP following the manufacturer's protocol and treated with A549 cells or HeLa cells. In the modified SM-102-LNP formulation, the only alteration was the substitution of the helper lipid DSPC with DOPE, while all other components remained unchanged. Subsequently, the transfected A549 or HeLa cells were observed by optical microscopy to confirm the EGFP expression after treatment for 24 h or 48 h. For HeLa cells, the molar ratios (ionizable lipid : phospholipid : PEG lipid : Rg2 or PPD) were further optimized to enhance the expression efficiency, resulting in a ratio of 50 : 10 : 0.75 : 39 for Rg2-LNP and 50 : 10 : 0.75 : 22.9 for PPD-LNP.

In addition, after 24 h of transfection, both cell lines were harvested and resuspended in PBS with 1% FBS and then the expression efficiency was evaluated by flow cytometry.

In vitro luciferase assay. A549 cells were treated with 250 ng of *Luc* mRNA encapsulated in LNPs, including commercial LNPs, Rg2-LNP, and PPD-LNP, to evaluate Luc expression. After 24 h of transfection, cells were harvested to passive lysis buffer and centrifuged at 12 000g for 10 min at 4 °C. The supernatant was then collected to measure relative luciferase activity using the luciferase assay system.

In vivo test for Luc mRNA delivery and expression. The animal experimental procedures followed the Guidelines for the Care and Use of Laboratory Animals of the Institute of Laboratory Animal Center, Daegu-Gyeongbuk Medical Innovation Foundation. All animal studies were approved by the Institutional Reviewer Board on the Ethics of Animal Experiments of the Daegu-Gyeongbuk Medical Innovation Foundation (approval number: KMEDI-24031903-00).

Male Balb/c nude mice were sacrificed to assess the efficiency of delivery and expression *in vivo*. Each mouse was dosed with 10 μg of *Luc* mRNA encapsulated in Rg2-LNP, PPD-LNP, SM-102-LNP, or modified SM-102-LNP through an intramuscular (I.M.) injection. The molar ratios of Rg2-LNP and PPD-LNP formulation used for the *Luc* mRNA *in vivo* delivery and expression tests were 50 : 10 : 0.75 : 39 and 50 : 10 : 0.75 : 22.9, respectively. The molar ratios of SM-102-LNP and modified SM-102-LNP formulations followed the manufacturer's protocol. For bioluminescence imaging (BLI), mice were administered D-luciferin *via* intraperitoneal injection. During imaging, anesthesia using 1–2% isoflurane gas was applied to all mice. BLI was conducted 5 min after substrate injection using the IVIS Lumina III imaging system, from 1 h to 54 h post-injection of *Luc* mRNA-encapsulated Rg2-LNP and PPD-LNP as well as SM-102-LNP and modified SM-102-LNP as the positive control. LIVING-IMAGE software (version 3.0, PerkinElmer) was utilized to overlay grayscale photographic images and bioluminescent color images. BLI signals were quantified in units of photons per cm^2 per second per steradian (P cm^{-2} s^{-1} sr^{-1}).

Statistical analysis. Data are presented as mean ± standard deviation (S.D.). Statistical analysis was conducted using one-way analysis of variance (ANOVA) with Tukey's test (OriginPro software, version 8.5), and statistically significant differences were defined as *$p < 0.05$, **$p < 0.01$, and ***$p < 0.001$.

Results and discussion

Characterization of Rg2-LNP and PPD-LNP

Following the preparation of Rg2-LNP and PPD-LNP, their physicochemical properties were characterized using various methods. The structural morphologies of Rg2-LNP, mRNA-Rg2-LNP, PPD-LNP and mRNA-PPD-LNP were observed by TEM after negative staining treatment with 2% uranyl acetate solution and they are depicted in Fig. 1 and Fig. S2.† Without mRNA, Rg2-LNP and PPD-LNP exhibited an empty vehicle structure (Fig. 1A and C). However, when mRNA was present, the structure of both LNPs changed clearly. Firstly, Rg2-LNP changed from a unilamellar to a multilamellar structure (Fig. 1A, B, and Fig. S2A†). This morphological transformation can be attributed to the amphiphilic properties of Rg2 and phospholipids, which facilitate self-assembly and enable the steroid part of Rg2 to adsorb into lipid bilayers within the LNPs.[41] Additionally, it was introduced that glucose could interact with guanin in nucleic acids *via* hydrogen bonding.[42] Another literature study reported that hydrogen bonds can form between the OH groups in glucose and the phosphate groups or nitrogenous bases in nucleotides, and this binding was characterized by FT-IR differential spectroscopy.[43] These studies suggest that the hydroxyl groups of glucose in Rg2 could create hydrogen bonds with the polar functional groups of mRNAs, such as the phosphate backbone or nitrogenous bases. Therefore, the relatively higher encapsulation rate of Rg2-LNP for mRNA could be due to these hydrogen bonds. On

the other hand, PPD-LNP transformed from an empty vehicle to a unilamellar structure with a nanostructured core in the presence of mRNA. This dark core indicates the self-assembly structure of mRNA, ionizable lipid, and helper lipid, which was negatively stained in the mRNA-PPD-LNP (Fig. 1D, E and Fig. S2B†). The structure of mRNA-PPD-LNP differs from that of mRNA-Rg2-LNP due to the hydrophobic properties of PPD, which interacts strongly with lipid structures. The average sizes of mRNA-Rg2-LNP and mRNA-PPD-LNP were measured by NTA to be around 117.3 ± 1.6 nm and 167.9 ± 3.9 nm, respectively (Fig. 1C and F). The sizes of the two LNPs were also measured using DLS. The average size of only Rg2-LNP was around 121 nm and mRNA-Rg2-LNP was approximately 132.9 nm, with a PDI of approximately 0.24, while the average size of PPD-LNP was about 144.7 nm and mRNA-PPD-LNP was approximately 168.9 nm, with a PDI of 0.26 (Fig. S2C and D†). In general, the presence of mRNA within the LNP structure leads to an increase in the overall size of the LNPs due to the additional payload. This occurs because mRNA can induce structural modifications, such as swelling or alterations in the arrangement of lipid layers. As a result, the size of both LNPs containing mRNA showed a slight increase. In addition, a PDI of 0.3 or less in the size measurement results indicates a homogeneous population of nanocarriers. Therefore, the two LNPs mentioned above are considered to have sufficient potential for use in drug delivery.[44,45] There was some difference between the size analysis results from NTA and DLS due to the different
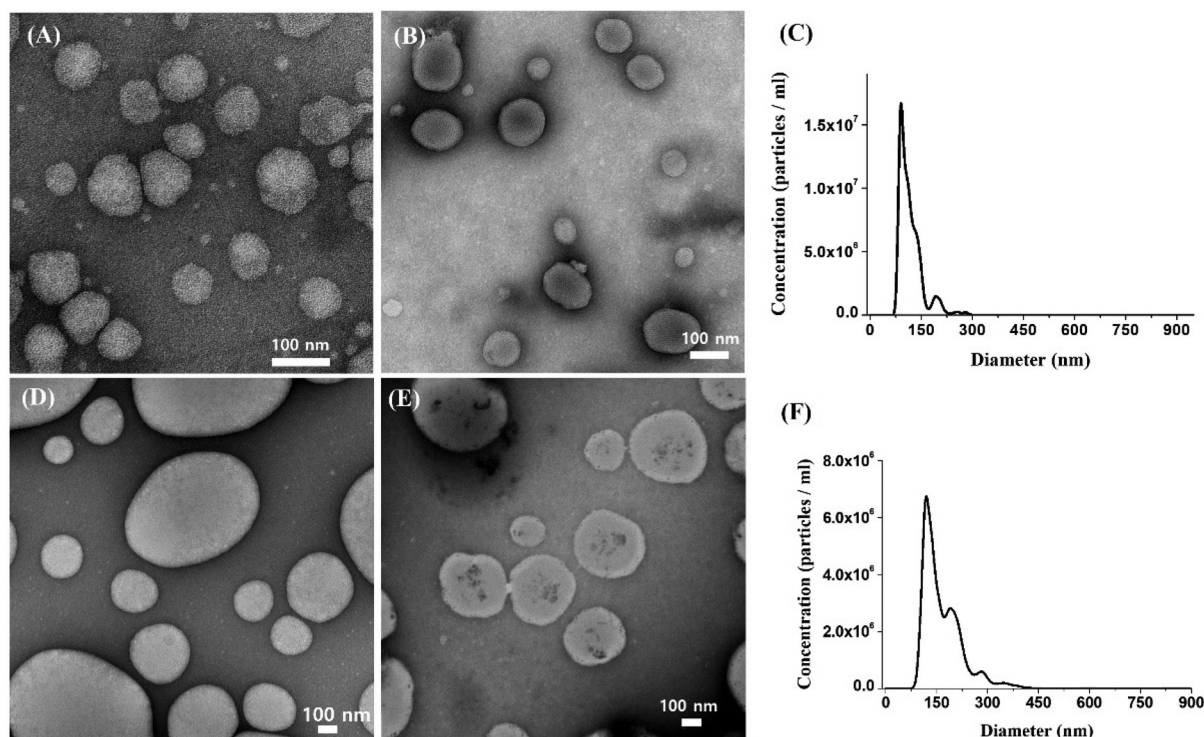
Fig. 1 TEM images of (A) Rg2–LNP, (B) EGFP mRNA–Rg2–LNP, (D) PPD–LNP, and (E) EGFP mRNA–PPD–LNP and NTA results of (C) EGFP mRNA–Rg2–LNP and (F) EGFP mRNA-PPD–LNP.

measurement mechanisms, but both sizes were suitable for functioning as LNP carriers.

Encapsulation efficiency and mRNA stability

The encapsulation efficiency of Rg2-LNP and PPD-LNP was evaluated using gel electrophoresis (Fig. 2A and C). For Rg2-LNP, no residual mRNA bands were observed at weight ratios of 1 : 10 and 1 : 20, indicating complete encapsulation. In contrast, PPD-LNP exhibited unencapsulated mRNA bands at all tested ratios (1 : 5, 1 : 10, and 1 : 20), though the band intensity decreased with increasing LNP mass. The encapsulation efficiency of Rg2-LNP and PPD-LNP was evaluated using the Ribogreen RNA assay, showing 81.9% and 68.7%, respectively. These mRNA-LNPs were prepared through simple hand mixing, which might result in a lower encapsulation efficiency compared to those prepared using a microfluidics system. Nevertheless, the Rg2-LNP and PPD-LNP produced by this mixing process were sufficient mRNA carriers for expressing EGFP and Luc for *in vitro* or *in vivo* experiments. However, we recognized the limitations of manual preparation, including challenges in achieving precise size uniformity and optimal mRNA encapsulation per LNP. To address these limitations, we plan to utilize microfluidic devices in future studies to enhance the development of mRNA-based therapeutics.

On the other hand, the higher encapsulation efficiency of Rg2-LNP can be attributed to the glucose component forming hydrogen bonds with mRNA and the ionizable lipid binding through electrostatic interactions, resulting in tighter mRNA capture, as mentioned above. mRNA stability within the LNPs was assessed by analyzing mRNA integrity after RNase treatment *via* electrophoresis (Fig. 2B and D). Naked mRNA was completely degraded by RNase exposure, whereas mRNA within Rg2-LNP and PPD-LNP remained intact even at increased RNase concentrations (red box in Fig. 2B and D). The unencapsulated mRNA band in PPD-LNP disappeared after RNase treatment, while the encapsulated mRNA remained protected, demonstrating that both Rg2-LNP and PPD-LNP effectively shield mRNA from degradation.

Biocompatibility of Rg2-LNP and PPD-LNP

The cytotoxicity of Rg2-LNP and PPD-LNP was evaluated using a CCK-8 assay (Fig. 3 and Fig. S3†). Treatment with 0.05 μg of Rg2-LNP and PPD-LNP reduced the number of A549 and HeLa cells by a maximum of 10%, with no significant changes in cell morphology (Fig. 3A and B). Furthermore, dose-dependent cytotoxicity was assessed, revealing no significant toxicity (Fig. S3†). Additionally, it should be noted that Rg2 and PPD are phytochemicals, and those are recognized as biologically active components derived from ginseng, known for its health benefits.[46–48] This suggests that the cytotoxicity of Rg2-LNP and PPD-LNP is minimal and not a critical concern for their application as gene delivery systems.

In vitro mRNA delivery and expression using Rg2-LNP and PPD-LNP vehicles

The delivery and translation efficiency of EGFP mRNA encapsulated in Rg2-LNP and PPD-LNP were evaluated in A549 and HeLa cells using various molar ratios of LNP components for optimization (Fig. S4†). From these assessments, the initial molar ratios for LNP formulation were determined to be 50 : 10 : 1.5 : 39 for Rg2-LNP and 50 : 10 : 1.5 : 22.9 for PPD-LNP. Firstly, in evaluating the delivery efficacy of LNPs, 250 ng of EGFP mRNA encapsulated by Rg2-LNP or PPD-LNP at a 1 : 10 weight ratio (mRNA : LNP) was transfected into A549 cells.
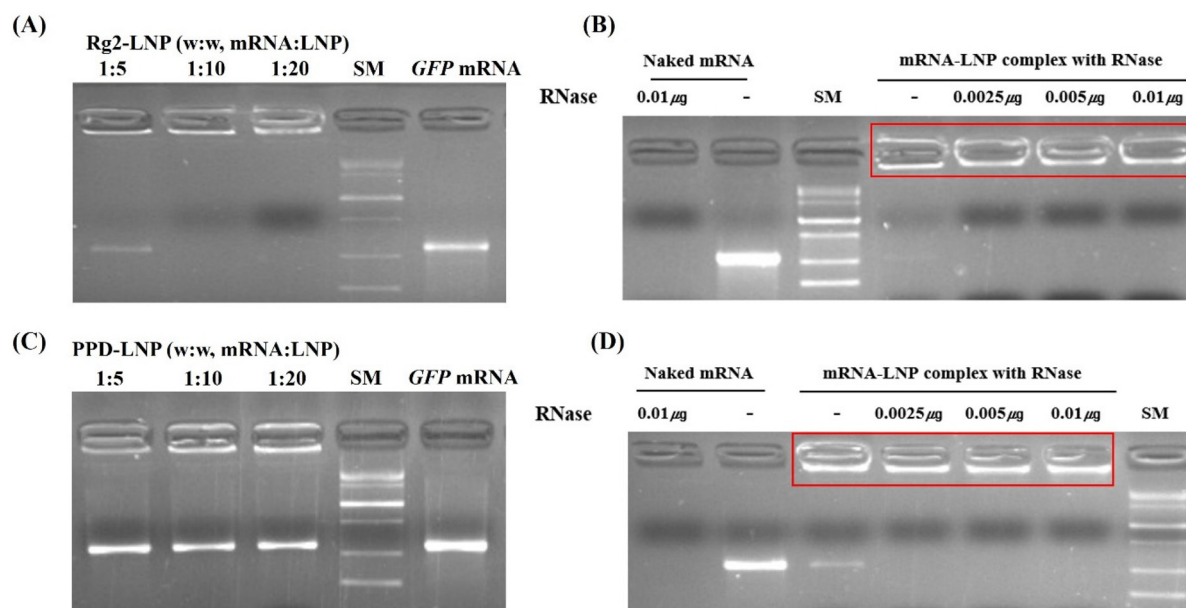

Fig. 2 Gel electrophoresis results of (A) Rg2-LNP and (C) PPD-LNP depending on the complexation mixing ratio for confirmation of mRNA encapsulation, and the results of the mRNA stability test against RNase of (B) EGFP mRNA-Rg2-LNP and (D) EGFP mRNA-PPD-LNP.
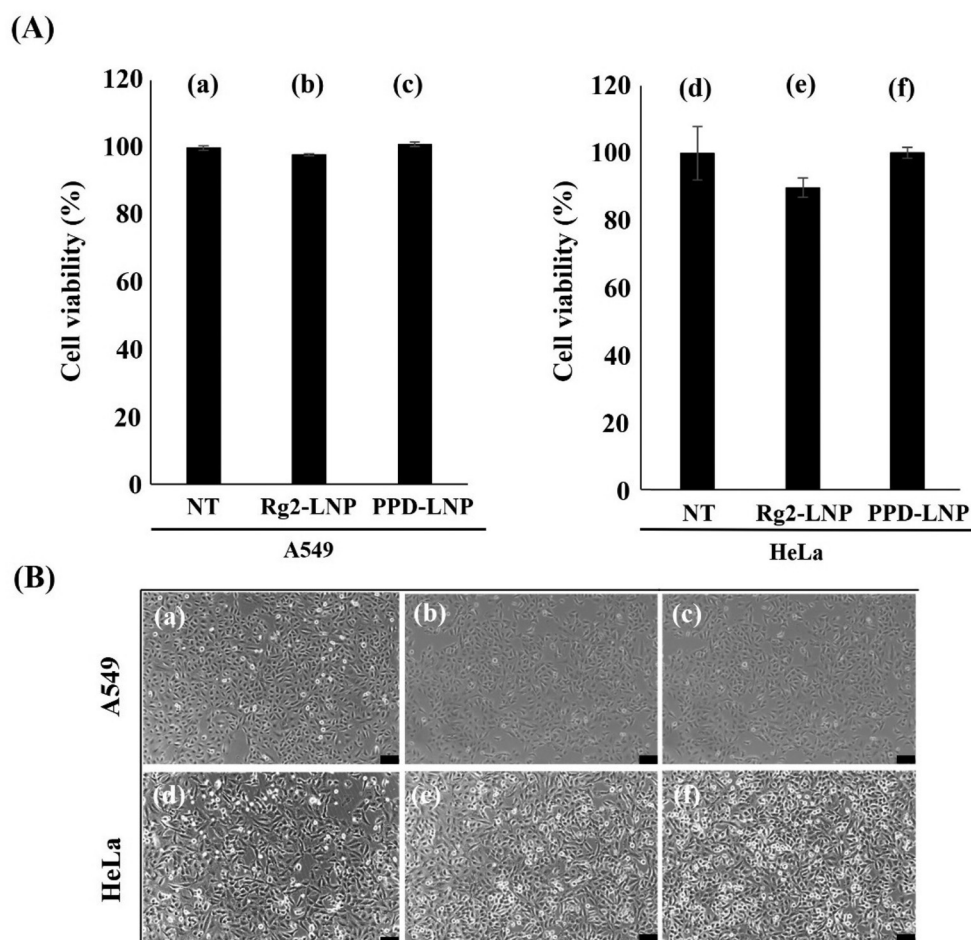
Fig. 3 Cytotoxicity profile of LNPs depending on the sterol structures. (A) Measurement of cell viability *via* cell counting kit-8 (CCK-8) assay and (B) microscopy images of cells after treatment of LNPs (scale bar: 100 μm).
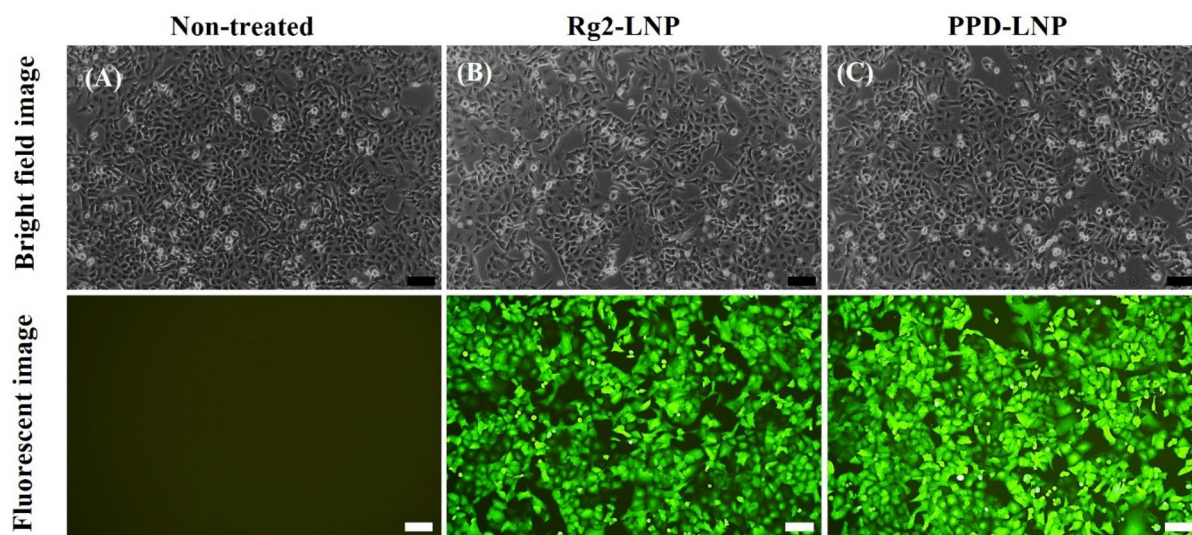
Fig. 4 Bright field images and fluorescence images of (A) non-treated, (B) EGFP mRNA-Rg2-LNP treated and (C) EGFP mRNA-PPD-LNP treated A549 cells (scale bar: 100 μm).

After 24 h of treatment, optical microscopy revealed a clear signal of green fluorescence in all treated cells, indicating successful delivery and translation of EGFP mRNA (Fig. 4B and C). Additionally, the delivery effectiveness and transfection efficiency of Rg2-LNP and PPD-LNP were compared with those of commercially available LNPs SM-102-LNP (Moderna) and ALC-0315-LNP (Pfizer/BioNTech), which retain the cholesterol component. After delivering EGFP mRNA with these LNPs, EGFP expression in A549 cells was carefully observed. According to the fluorescence image, the fluorescence brightness was significantly higher in cells transfected with Rg2-LNP and PPD-LNP compared to those of SM-102-LNP and ALC-0315-LNP (Fig. S5A†). In addition, the efficiency of EGFP expression was compared by flow cytometry with various LNP carriers (Fig. S5B–D†). In this case, the population of EGFP-positive A549 cells was over 95% after treatment with EGFP

mRNA encapsulated Rg2-LNP, PPD-LNP, and SM-102-LNP, but it was only 25% in ALC-0315-LNP. Interestingly, the mean fluorescence intensity (MFI) was the highest in the case of PPD-LNP, followed by Rg2-LNP, which was higher than SM-102-LNP. In addition, *Luc* mRNA transfection yields were compared between commercial LNPs and Rg2-LNP and PPD-LNP in A549 cell lines using a bioluminescence assay (Fig. S6†). The results were similar to those of the EGFP expression trends in that relative light units (RLU) were higher for Rg2-LNP and PPD-LNP compared to SM-102-LNP and ALC-0315-LNP. Additionally, the *GFP* mRNA delivery and expression efficiency of modified SM-102-LNP, where the helper lipid was switched from DSPC to DOPE, was compared with Rg2-LNP and PPD-LNP, and the results are presented in Fig. S7.† In this case, brighter green fluorescence was observed in LNPs based on SM-102/DOPE/Rg2/PEG lipid (Rg2-LNP) or SM-102/DOPE/PPD/PEG lipid (PPD-LNP)
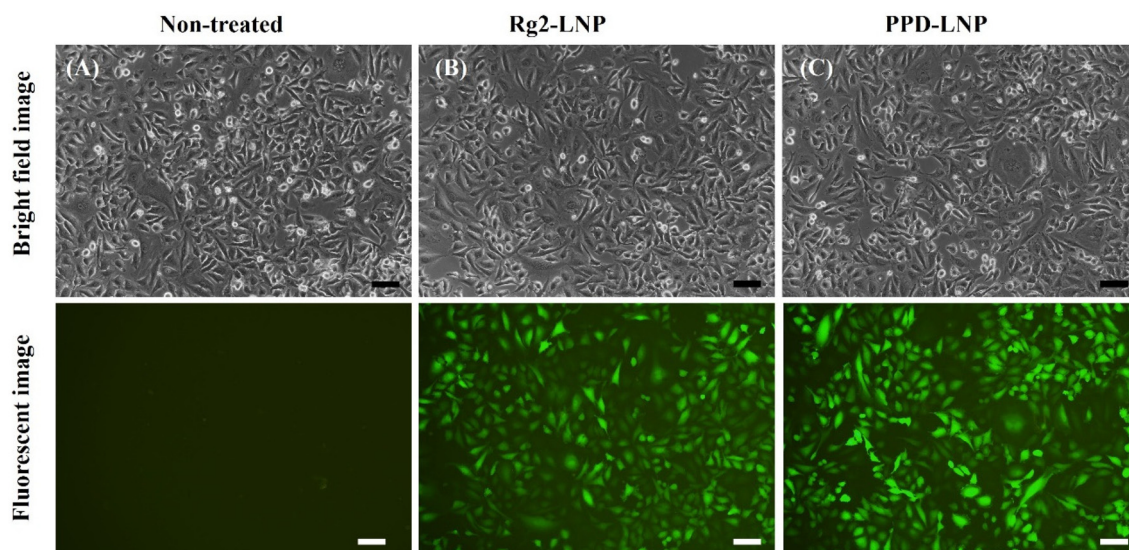

Fig. 5 Observation of EGFP expression in HeLa cells. (A) Non-treated conditions, (B) EGFP mRNA-Rg2-LNP conditions and (C) EGFP mRNA-PPD-LNP conditions (scale bar: 100 μm).
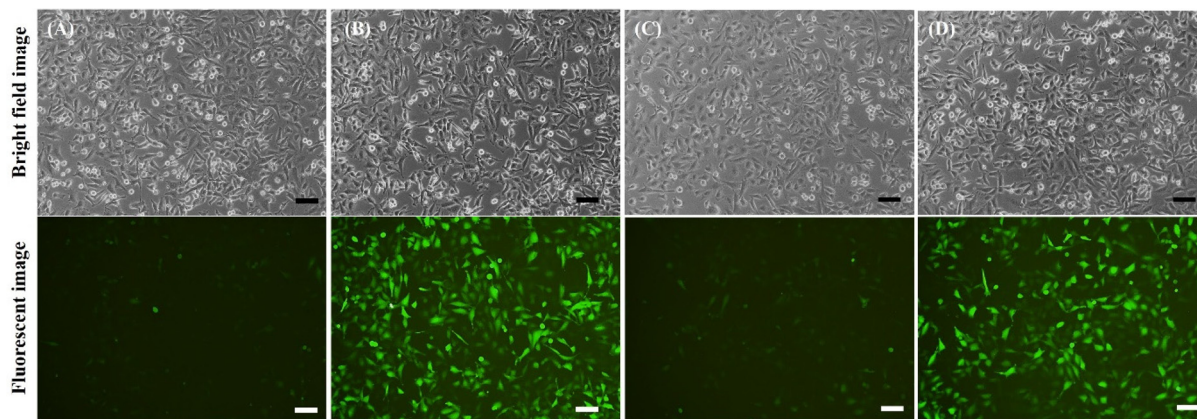

Fig. 6 Observation of EGFP expression to optimize the weight ratio between mRNA and LNP in HeLa cells (mRNA : LNP = w : w); (A) 1 : 10 and (B) 1 : 20 in EGFP mRNA-Rg2-LNP, and (C) 1 : 10 and (D) 1 : 20 in EGFP mRNA-PPD-LNP (scale bar: 100 μm).

than in LNPs formulated with SM-102/DOPE/cholesterol/PEG lipid (modified SM-102 LNP).

Optimization of mRNA delivery and transfection

EGFP mRNA encapsulated in Rg2-LNP and PPD-LNP were also treated with HeLa cells, resulting in observable green fluorescence (Fig. 5B and C). The expression of EGFP in HeLa cells was critically influenced by the weight ratio (mRNA : LNP) at 1 : 10 and 1 : 20, and a higher signal intensity of EGFP was observed at a 1 : 20 weight ratio (mRNA : LNP) instead of 1 : 10 (Fig. 6). Interestingly, when assessing the encapsulation

efficiency of LNPs by gel electrophoresis, results showed that nearly all mRNA was encapsulated in Rg2-LNP at 1 : 10 and 1 : 20 ratios, and for PPD-LNP, unencapsulated mRNA bands were similar at both ratios, so it was expected that the tendency of EGFP expression might be the same for both weight ratios in HeLa cells as in A549 cells. This indicates that the tendency of expression efficiency did not directly correspond to the encapsulation efficiency. The expression efficiency and MFI of EGFP in HeLa cells were also evaluated after transfection of EGFP mRNA using commercial LNPs, Rg2-LNP, and PPD-LNP, similar to the tests conducted in A549 cells. Flow cytometry
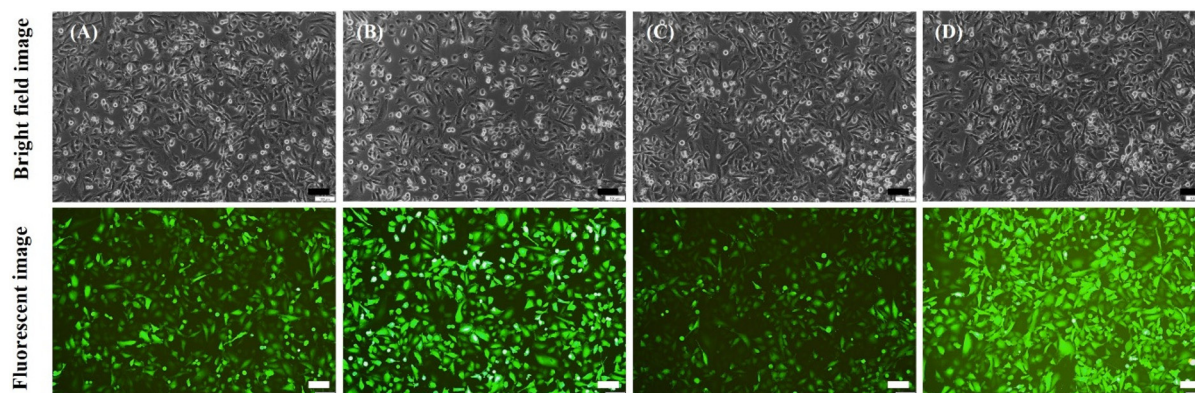
Fig. 7 Monitoring of the EGFP expression efficiency depending on the molar ratio of PEG lipid in the LNP formulation (molar ratio = ionizable lipid : phospholipid : PEG lipid : Rg2 or PPD). (A) 50 : 10 : 1.5 : 39 and (B) 50 : 10 : 0.75 : 39 of Rg2-LNP with EGFP mRNA as well as (C) 50 : 10 : 1.5 : 22.9 and (D) 50 : 10 : 0.75 : 22.9 of PPD-LNP with EGFP mRNA (after treatment for 24 h, scale bar: 100 μm).

Potential of *in vivo* mRNA delivery and expression
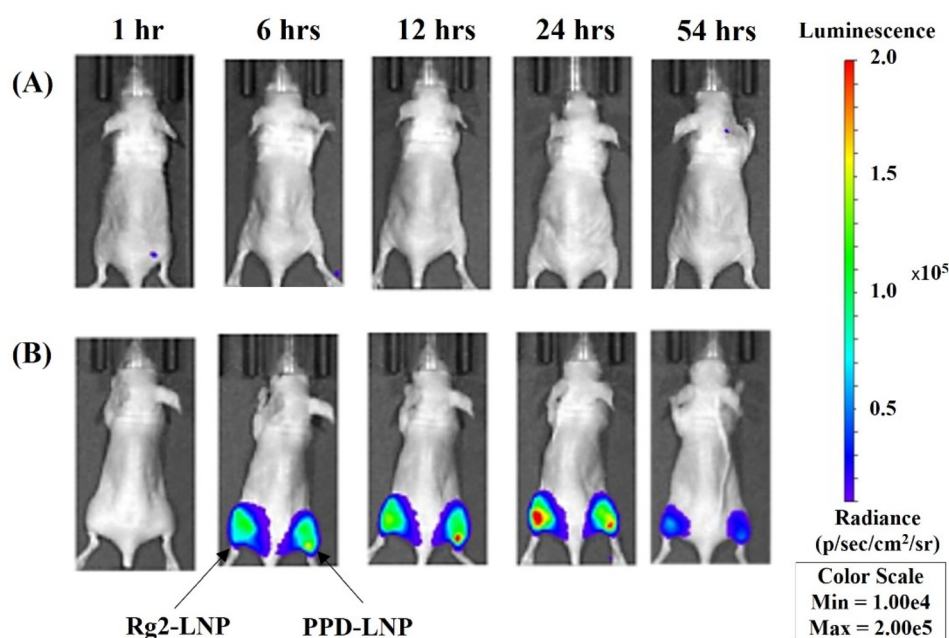
Fig. 8 *In vivo* monitoring of luciferase expression following intramuscular (I.M.) injection of *luciferase* mRNA encapsulated Rg2-LNP and PPD-LNP in nude mice (n = 3, injected mRNA dose = 10 μg). Bioluminescence imaging in (A) non-treated (vehicle) mice and (B) *Luc* mRNA encapsulated Rg2-LNP and PPD-LNP (*Luc* mRNA-Rg2-LNP and *Luc* mRNA-PPD-LNP) injected mice.

analysis results showed that although the expression efficiency and MFI were lower in HeLa cells compared to A549 cells, PPD-LNP had the highest MFI, demonstrating a similar pattern in HeLa cells (Fig. S8†). This finding indicates that the newly developed LNPs have excellent transfection efficiency. Also, the results highlight the importance of tuning and optimizing formulation conditions for effective protein expression in target cell lines.

Additional optimization involved reducing the PEG lipid component in the LNP formulation, which enhanced the EGFP translation efficiency (Fig. 7B and D). It was reported that a lower surface density of PEG has been associated with increased uptake into cancer cells, including HeLa cells.[49–51] In our case, also a lower PEG density improved lipid nanoparticle uptake by HeLa cells, thereby increasing EGFP translation. Furthermore, high levels of EGFP expression remained after 48 h post-treatment (Fig. S9†). These findings emphasize optimizing the mRNA : LNP weight ratio and the PEG lipid content based on the target cell type to achieve delivery and optimal translation efficiency.

Potential of *in vivo* mRNA delivery and expression

The potential for *in vivo* applications of Rg2-LNP and PPD-LNP was assessed using bioluminescence imaging in mice. Mice were intramuscularly injected with *Luc* mRNA encapsulated in Rg2-LNP and PPD-LNP. The bioluminescence imaging revealed a signal of *Luc* mRNA translation at 6 hours post-injection, which persisted until 54 h (Fig. 8B, Fig. S10 and S11†), while no evident signal from empty vehicles was present. To evaluate the efficiency of *in vivo* mRNA delivery and expression in cells of mRNA encapsulated in LNPs, Rg2-LNP, and PPD-LNP, mRNA-Luc expression was examined in hairless mice. Commercially available cholesterol-retaining SM-102-LNP (with DSPC as the helper lipid) and modified SM-102-LNP (with DOPE as the helper lipid) were used as positive controls because the population of EGFP-positive cells was comparable between SM-102-LNP, Rg2-LNP, and PPD-LNP, SM-102-LNP. According to IVIS imaging and total flux profiles after I.M. injection, the total flux of the SM-102-LNP series decreased rapidly after 6 hours (Fig. S10 and S11†).

In contrast, the expression pattern of Luc in Rg2-LNP and PPD-LNP showed a slightly delayed initial expression compared to that of SM-102-LNP, but the decrease in Luc expression was slower. Notably, Rg2-LNP had the highest flux value after 12 hours post-injection across all LNP conditions according to the profile of total flux. Additionally, the total flux of PPD-LNP was higher than that of SM-102-LNP at 12 hours post-injection (Fig. S11†). These results unequivocally demonstrate the effectiveness of Rg2-LNP and PPD-LNP in delivering mRNA and facilitating translation *in vivo*, instilling confidence in their potential for gene therapy applications.

lipid nanoparticles (LNPs) incorporating ginsenoside Rg2 and its derivative PPD as sterol components, replacing cholesterol in the LNP formulation. The formulation was optimized by adjusting the molar ratio of lipid components to Rg2 or PPD and the weight ratio between mRNA and LNP. The Rg2-LNP and PPD-LNP were prepared manually through a simple mixing method, resulting in highly dispersed spherical LNPs. These carriers exhibited low toxicity, good encapsulation efficiency, and strong mRNA protection ability. Flow cytometry analysis revealed that transfection with Rg2-LNP or PPD-LNP encapsulating EGFP mRNA resulted in significantly higher transfection efficiency and MFI in A549 and HeLa cells compared to commercially available LNPs. Furthermore, evaluating mRNA delivery and expression of LNPs encapsulating *Luc* mRNA using hairless mice indicated that these LNPs possessed high delivery efficiency *in vivo* as well.

In conclusion, the mRNA complexes with Rg2-LNP or PPD-LNP, synthesized through a straightforward manual mixing process, demonstrated highly effective mRNA delivery and expression, highlighting their potential as robust mRNA delivery systems in this study.

Author contributions

Sin A Park: methodology, investigation, formal analysis, and writing – original draft. Dajeong Hwang: methodology, investigation, formal analysis, and writing – original draft. Jae Hoon Kim: investigation and formal analysis. Seung-Yeul Lee: investigation and formal analysis. Jaebeom Lee: investigation, resource, and writing – review and editing. Han Sang Kim: resource, investigation, resource, and writing – review and editing. Kyung-A Kim: investigation and writing – review and editing. Bumhee Lim: resource, formal analysis, and writing – review and editing. Jae-Eon Lee: investigation, formal analysis, and writing – original draft. Yong Hyun Jeon: resource, methodology, formal analysis, and writing – review and editing. Tae Jeong Oh: project administration and writing – review and editing. Jaewook Lee: conception, methodology, investigation, formal analysis, visualization, writing – original draft, and writing – review and editing. Sungwhan An: supervision, project administration, conception, writing – original draft, and writing – review and editing.

Data availability

All data are saved and located in the Network Attached Storage (NAS) system of Genomictree, and due to the confidentiality of data, the data including raw files used or analyzed during the current study are available from the corresponding authors on reasonable request.

Conclusion

As mRNA-based therapeutics expand, developing suitable carriers has become increasingly important. This study developed

Conflicts of interest

The authors S. A. Park, D. Hwang, J. H. Kim, S.-Y. Lee, T. J. Oh, J. Lee and S. An were employed by the company Genomictree,

Inc, and T. J. Oh and S. An are shareholders of Genomictree, Inc. The authors S. An and J. Lee are inventors on patent applications currently pending related to the content of this manuscript. The remaining authors declare that the research was conducted in the absence of any commercial or financial relationships that could be construed as a potential conflict of interest.

Acknowledgements

References

1 S. Ke, A. Pandya-Jones, Y. Saito, J. J. Fak, C. B. Vågbø, S. Geula, J. H. Hanna, D. L. Black, J. E. Darnell and R. B. Darnell, *Genes Dev.*, 2017, **31**, 990–1006.

2 A. Li, Y.-S. Chen, X.-L. Ping, X. Yang, W. Xiao, Y. Yang, H.-Y. Sun, Q. Zhu, P. Baidya, X. Wang, D. P. Bhattarai, Y.-L. Zhao, B.-F. Sun and Y.-G. Yang, *Cell Res.*, 2017, **27**, 444–447.

3 D. M. Mauger, B. J. Cabral, V. Presnyak, S. V. Su, D. W. Reid, B. Goodman, K. Link, N. Khatwani, J. Reynders, M. J. Moore and I. J. McFadyen, *Proc. Natl. Acad. Sci. U. S. A.*, 2019, **116**, 24075–24083.

4 G. Tavernier, O. Andries, J. Demeester, N. N. Sanders, S. C. De Smedt and J. Rejman, *J. Controlled Release*, 2011, **150**, 238–247.

5 Z. Meng, J. O'Keeffe-Ahern, J. Lyu, L. Pierucci, D. Zhou and W. Wang, *Biomater. Sci.*, 2017, **5**, 2381–2392.

6 C. E. Dunbar, K. A. High, J. K. Joung, D. B. Kohn, K. Ozawa and M. Sadelain, *Science*, 2018, **359**, eaan4672.

7 N. Chaudhary, D. Weissman and K. A. Whitehead, *Nat. Rev. Drug Discovery*, 2021, **20**, 817–838.

8 J. Lutz, S. Lazzaro, M. Habbeddine, K. E. Schmidt, P. Baumhof, B. L. Mui, Y. K. Tam, T. D. Madden, M. J. Hope, R. Heidenreich and M. Fotin-Mleczek, *npj Vaccines*, 2017, **2**, 29.

9 S. S. Rosa, D. M. F. Prazeres, A. M. Azevedo and M. P. C. Marques, *Vaccine*, 2021, **39**, 2190–2200.

10 J. Chen, J. Chen and Q. Xu, *Annu. Rev. Biomed. Eng.*, 2022, **24**, 85–109.

11 J. Lee, J.-H. Lee, K. Chakraborty, J. Hwang and Y.-K. Lee, *RSC Adv.*, 2022, **12**, 18475–18492.

12 D. Mishra, J. R. Hubenak and A. B. Mathur, *J. Biomed. Mater. Res., Part A*, 2013, **101**, 3646–3660.

13 C. Bharti, U. Nagaich, A. K. Pal and N. Gulati, *Int. J. Pharm. Invest.*, 2015, **5**, 124–133.

14 V. Sokolova and M. Epple, *Angew. Chem., Int. Ed.*, 2008, **47**, 1382–1395.

15 C. Heneweer, S. E. Gendy and O. Peñate-Medina, *Ther. Delivery*, 2012, **3**, 645–656.

16 A. Luchini and G. Vitiello, *Front. Chem.*, 2019, **7**, 343.

17 P. R. Cullis and M. J. Hope, *Mol. Ther.*, 2017, **25**, 1467–1475.

18 J. A. Kulkarni, D. Witzigmann, S. Chen, P. R. Cullis and R. van der Meel, *Acc. Chem. Res.*, 2019, **52**, 2435–2444.

19 Y. Zhao and L. Huang, in *Advances in Genetics*, ed. L. Huang, D. Liu and E. Wagner, Academic Press, 2014, vol. 88, pp. 13–36.

20 J. E. N. Dolatabadi, H. Valizadeh and H. Hamishehkar, *Adv. Pharm. Bull.*, 2015, **5**, 151–159.

21 X. Hou, T. Zaks, R. Langer and Y. Dong, *Nat. Rev. Mater.*, 2021, **6**, 1078–1094.

22 L. Schoenmaker, D. Witzigmann, J. A. Kulkarni, R. Verbeke, G. Kersten, W. Jiskoot and D. J. A. Crommelin, *Int. J. Pharm.*, 2021, **601**, 120586.

23 J. C. Kraft, J. P. Freeling, Z. Wang and R. J. Y. Ho, *J. Pharm. Sci.*, 2014, **103**, 29–52.

24 F. Ding, H. Zhang, J. Cui, Q. Li and C. Yang, *Biomater. Sci.*, 2021, **9**, 7534–7546.

25 A. Valenzuela, J. Sanhueza and S. Nieto, *Biol. Res.*, 2003, **36**, 291–302.

26 W. Kulig, L. Cwiklik, P. Jurkiewicz, T. Rog and I. Vattulainen, *Chem. Phys. Lipids*, 2016, **199**, 144–160.

27 G. Leonarduzzi, B. Sottero and G. Poli, *J. Nutr. Biochem.*, 2002, **13**, 700–710.

28 Y. Song, J. Liu, K. Zhao, L. Gao and J. Zhao, *Cell Metab.*, 2021, **33**, 1911–1925.

29 M. K. Pulfer and R. C. Murphy, *J. Biol. Chem.*, 2004, **279**, 26331–26338.

30 V. M. Olkkonen, O. Béaslas and E. Nissilä, *Biomolecules*, 2012, **2**, 76–103.

31 J. C. Verhagen, P. ter Braake, J. Teunissen, G. van Ginkel and A. Sevanian, *J. Lipid Res.*, 1996, **37**, 1488–1502.

32 D. W. Jayme and S. R. Smith, *Cytotechnology*, 2000, **33**, 27–36.

33 R. Conte, V. Marturano, G. Peluso, A. Calarco and P. Cerruti, *Int. J. Mol. Sci.*, 2017, **18**, 709.

34 D. Sun, S.-Y. Guo, L. Yang, Y.-R. Wang, X.-H. Wei, S. Song, Y.-W. Yang, Y. Gan and Z.-T. Wang, *Acta Pharmacol. Sin.*, 2020, **41**, 119–128.

35 X.-R. Tan, L. Chao, K.-K. Feng, J.-Q. Le, J.-W. Shen and J.-W. Shao, *J. Ind. Eng. Chem.*, 2022, **116**, 303–309.

36 X. Zhao, J. Wu, K. Zhang, D. Guo, L. Hong, X. Chen, B. Wang and Y. Song, *Nanoscale Adv.*, 2022, **4**, 190–199.

37 A. Vijayakumar, R. Baskaran, J.-H. Baek, P. Sundaramoorthy and B. K. Yoo, *AAPS PharmSciTech*, 2019, **20**, 88.

38 X. Song, L. Zang and S. Hu, *Vaccine*, 2009, **27**, 2306–2311.

39 C. Yue, D. Li, S. Fan, F. Tao, Y. Yu, W. Lu, Q. Chen, A. Yuan, J. Wu, G. Zhao, H. Dong and Y. Hu, *Biomaterials*, 2023, **301**, 122291.

40 S. An, *Republic of Korea Pat*, 10-2021-0137521, 2021.

41 S. L. Verstraeten, J. H. Lorent and M.-P. Mingeot-Leclercq, *Front. Pharmacol.*, 2020, **11**, 576887.

42 E. Vengut-Climent, I. Gómez-Pinto, R. Lucas, P. Peñalver, A. Aviñó, C. Fonseca Guerra, F. M. Bickelhaupt, R. Eritja, C. González and J. C. Morales, *Angew. Chem., Int. Ed.*, 2016, **55**, 8643–8647.

43 L. El-Mahdaoui, J. F. Neault and H. A. Tajmir-Riahi, *J. Inorg. Biochem.*, 1997, **65**, 123–131.

44 M. Danaei, M. Dehghankhold, S. Ataei, F. Hasanzadeh Davarani, R. Javanmard, A. Dokhani, S. Khorasani and M. R. Mozafari, *Pharmaceutics*, 2018, **10**, 57.

45 L. Xu, X. Wang, Y. Liu, G. Yang, R. J. Falconer and C.-X. Zhao, *Adv. NanoBiomed Res.*, 2022, **2**, 2100109.

46 Z. A. Ratan, M. F. Haidere, Y. H. Hong, S. H. Park, J.-O. Lee, J. Lee and J. Y. Cho, *J. Ginseng Res.*, 2021, **45**, 199–210.

47 D. L. Huynh, N. H. Nguyen and C. T. Nguyen, *Mol. Cell. Biochem.*, 2021, **476**, 3329–3340.

48 S. Zhang, B. Zheng, Y. Wei, Y. Liu, L. Yang, Y. Qiu, J. Su and M. Qiu, *Biomater. Sci.*, 2024, **12**, 2672–2688.

49 S. Hak, E. Helgesen, H. H. Hektoen, E. M. Huuse, P. A. Jarzyna, W. J. M. Mulder, O. Haraldseth and C. D. L. Davies, *ACS Nano*, 2012, **6**, 5648–5658.

50 D. Pozzi, V. Colapicchioni, G. Caracciolo, S. Piovesana, A. L. Capriotti, S. Palchetti, S. De Grossi, A. Riccioli, H. Amenitsch and A. Laganà, *Nanoscale*, 2014, **6**, 2782–2792.

51 C. Cruje and D. B. Chithrani, *J. Nanomed. Res.*, 2014, **1**, 27–32.